IAU 8th Asia-Pacific Regional Meeting
ASP Conference Series, Vol. nnn, 2003
S. Ikeuchi, J. Hearnshaw & T. Hanawa, eds.

Progress on Numerical Simulations of Solar Flares and Coronal Mass Ejections

Kazunari Shibata

Kwasan Observatory, Kyoto University, Yamashina, Kyoto 607-8471, Japan

Abstract. Recent progress of numerical simulations of solar flares and coronal mass ejections is discussed with emphasis on MHD simulations of magnetic reconnection and their application to recent space observations such as those by Yohkoh.

1. Introduction

Now is the golden age of solar observations. Recent space observations of the Sun with Yohkoh, SOHO, and TRACE have made a revolution in solar physics, and revealed that the magnetic field, especially its non-steady dynamics associated with reconnection, plays a central role in the production of flares and coronal mass ejections (CMEs). Since these non-steady dynamics are well described by magnetohydrodynamic (MHD) equations, we have to solve non-steady (resistive) MHD equations to understand the basic physics of flares and CMEs. This is practically impossible with an analytical approach, because of the intrinsic non-linearity of MHD equations. Thus the only way to attack this problem is by the numerical approach. Recent rapid progress in computers has enabled us for the first time to simulate these complicated non-linear, non-steady MHD processes in flares and CMEs in a realistic situation. From this point of view, we are now also in the golden age of solar MHD simulations: we can now compare excellent observational movies (e.g., Yohkoh X-ray movies) with MHD simulation movies, so that we can discuss the physics of flares and CMEs quantitatively and in detail, and we can even estimate unobservable quantities from such a comparison.

In this article, we first briefly review recent developments in the observation of solar flares and CMEs by spacecraft, in particular by Yohkoh, and then discuss recent progress of numerical simulations of solar flares and CMEs, with emphasis on MHD reconnection and applications to these observations.

2. Observations of Flares and Coronal Mass Ejections

Recent space observations have revealed a variety of evidence for reconnection in flares and the solar corona, such as cusp-shaped loops, loop top hard X-ray sources, giant arcades, plasmoid ejections, X-ray jets, and so on (e.g., see Tsuneta 1996; Shibata 1999; Aschwanden et al. 2001 and references therein).

It has also been revealed that plasmoid (or flux rope) ejections are much more common in flares than had been thought, and that not only LDE (long duration event) flares but also impulsive flares are very similar to CME-related flares. On the other hand, it has been found that many non-flare CMEs are associated with giant arcades, which are physically quite similar to cusp-shaped flare loops/arcades. Even tiny microflares or nanoflares often produce X-ray jets, Hα surges, or EUV jets.

Table 1. Comparison of various "flares"

"frare"	micro-flares	implusive flares	LDE flares	giant arcades
size (L) (10^4 km)	$0.5-4$	$1-10$	$10-40$	$30-100$
time scale (t) (s)	$60-600$	$60-3\times10^3$	$3\times10^3-10^5$	$10^4-2\times10^5$
energy (erg)	$10^{26}-10^{29}$	$10^{29}-10^{32}$	$10^{30}-10^{32}$	$10^{29}-10^{32}$
mass ejection	X-ray jet/ H_α surge	X-ray/H_α filament eruption	X-ray/H_α filament eruption	X-ray/H_α filament eruption
B (G)	100	100	30	10
n_e (cm^{-3})	10^{10}	10^{10}	2×10^9	3×10^8
V_A (km s^{-1})	3000	3000	2000	1500
$t_A = L/V_A$	5	10	90	400
t/t_A	$12-120$	$6-300$	$30-10^3$	$25-500$

Hence, a unified view has emerged from these new observations (Table I), and unified model has been proposed (Shibata 1999). Though the total energy of these "flares" ranges widely, from 10^{26} ergs for microflares to 10^{32} ergs for LDE flares and giant arcades, it is easy to explain such an observed variation of "flare" energies by the stored magnetic energy in a corresponding flare volume $E_{\rm flare} \simeq \frac{B^2}{8\pi}L^3 \simeq 4\times10^{32}\left(\frac{B}{100\ {\rm G}}\right)^2\left(\frac{L}{10^{10}\ {\rm cm}}\right)^3$ erg, where B is the average magnetic field strength in a flare volume with a characteristic length L. The time scale of flares shows an even wider dynamic range; i.e., from a few tens of seconds for microflares, to a few days for giant arcades associated with CMEs. However, if we normalize the time scale by the Alfven time $t_A = L/V_A$, all time scales of various "flares" become comparable to 10–1000. (In other words, the non-dimensional reconnection rate is 0.001–0.1.)

Furthermore, the observations of ubiquity of plasmoid (flux rope) ejections suggest the concept of *plasmoid-induced-reconnection* (Shibata and Tanuma 2001), in which magnetic reconnection is strongly coupled with plasmoid ejections, because of the following two roles of plasmoids in reconnection: i.e., (1) to store energy by inhibiting reconnection, and (2) to induce strong inflow into the reconnection region when plasmoids are ejected out of the current sheet. This, as well as the highly time dependent behavior of flare emissions in hard X-rays and microwaves, further suggests the *fractal reconnection* (Tajima and Shibata 1997, Shibata and Tanuma 2001), in which many plasmoids (flux ropes

or filaments) with different size are created in a current sheet, and are coalesced into each other and ejected out of the sheet to induce reconnection with various size and time scales. This is favorable to connect on a macro-scale ($\sim 10^9$ cm) and on a micro-scale ($\sim$ 100 cm) where anomalous resistivity or collisionless conductivity can eventually work.

3. Simulations of Magnetic Reconnection

At first, we should remember that it is still not possible to take fully realistic physical parameters for modelling solar flares and CMEs with present numerical simulations. The biggest difficulty is in the magnetic Reynolds number $R_{\rm m} = LV_{\rm A}/\eta \sim 10^{13}$ for classical Spitzer resistivity and typical coronal conditions, $L = 10^9$ cm, $V_{\rm A} = 10^8$ cm/s, and $\eta \sim 10^4$ cm^2/s (for $T = 10^6$ K). With the present supercomputers, the maximum magnetic Reynolds number in simulations is of the order of $10^3 - 10^4$. Thus there is a huge gap between realistic and numerical magnetic Reynolds numbers.

One of the recent achievements in numerical simulations of magnetic reconnection is the following: *If uniform resistivity is assumed, the magnetic reconnection becomes the Sweet-Parker type, i.e., slow reconnection with a time scale* $t_{\rm Sweet-Parker} \simeq R_{\rm m}^{1/2} t_{\rm A}$. *In order to get fast reconnection such as Petschek type,* $t_{\rm Petschek} \simeq 10 - 100 R_{\rm m}^0 t_{\rm A}$, *we need to assume spatially localized resistivity.* (Biskamp 1986, Scholer 1989, Ugai 1992, Yokoyama and Shibata 1994, Schumacher and Kliem 1996, Magara and Shibata 1999). The so called anomalous resistivity model, $\eta = \eta_0 |v_{\rm d} - v_{\rm c}|$ (for $v_{\rm d} = j/\rho > v_{\rm c}$) and otherwise $\eta = 0$, satisfies this condition.

4. Simulations of Solar Flares and CMEs

4.1. Reconnection Driven by Emerging Flux

Shibata, Nozawa, and Matsumoto (1992) carried out time-dependent MHD numerical simulations of reconnection occurring in a current sheet between an emerging flux and a pre-existing horizontal coronal magnetic field, by assuming the anomalous resistivity model and self-consistent emerging flux model (as a result of the Parker instability). They found that the reconnection proceeds in a very time-dependent manner: The tearing instability occurs in the current sheet, creating magnetic islands (plasmoids). These islands coalesce with each other, making bigger and bigger islands (plasmoids), and are eventually ejected out of the sheet. After the plasmoid ejection, the Petschek-type fast reconnection occurs. They predicted coexistence of both cool and hot plasma ejections.

Yokoyama and Shibata (1995, 1996) extended this simulation significantly. They studied both horizontal and oblique field cases for coronal magnetic field geometry, and confirmed that the basic physics is common in both cases. They found that not only hot jets but also cool jets are accelerated (Fig. 1), and predicted the coexistence of both X-ray jets and Hα surges. Indeed, such coexistence of both jets has been found by simultaneous observations by Yohkoh and ground based Hα observations (Canfield et al. 1996).

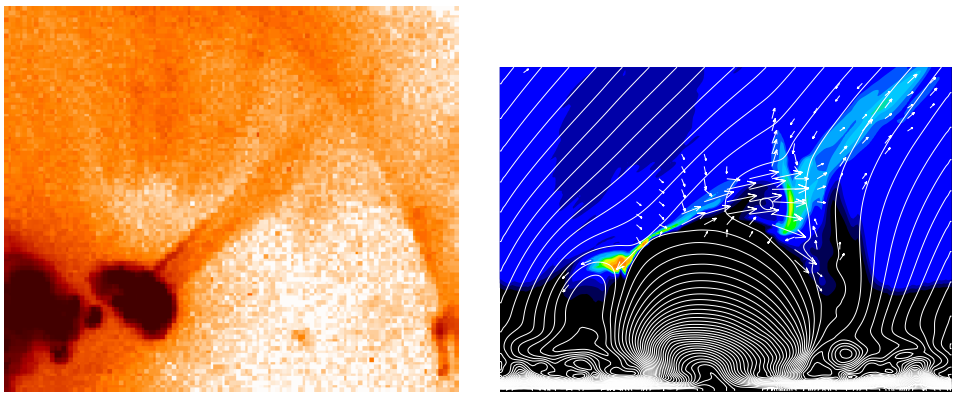

Figure 1. left: X-ray jet observed with the Yohkoh soft X-ray telescope (Shibata et al. 1992). Right: MHD simulation of X-ray jet (Yokoyama and Shibata 1995, 1996). The color map shows the temperature distribution.

4.2. Effect of Heat Conduction

The typical flare temperature is of order of 10^7 K. In such a high temperature, the conduction cooling time becomes very short:

$$t_{\rm cond} \simeq \frac{3nkTL^2}{\kappa_0 T^{5/2}} \simeq 1.3 \text{ s } \left(\frac{T}{10^7 \text{ K}}\right)^{-5/2} \left(\frac{n}{10^9 \text{ cm}^{-3}}\right) \left(\frac{L}{10^9 \text{ cm}}\right)^2, \qquad (1)$$

whereas the radiative cooling time is much longer ($\sim 10^5$ s for flare plasma in the early phase with $T \sim 10^7$ K, $n \sim 10^9$ cm^{-3}). Here, $\kappa_0 \simeq 10^{-6}$ is Spitzer's thermal conductivity along magnetic field lines. The Alfven time, $t_{\rm A} \simeq L/V_{\rm A} \sim 10$ s, is longer than the conduction cooling time. Hence, the heat conduction is very important in the dynamics and thermodynamics of flare plasma. In particular, the heat conduction causes *chromospheric evaporation* (ablation of dense chromospheric plasma), providing flare loops with hot dense plasma, which becomes the source of strong soft X-ray emission. If we want to model soft X-ray emission from flare loops, we have to take into account heat conduction and chromospheric evaporation, as already studied by one-dimensional flare loop modelling (e.g., Hori et al. (1997) for a flare loop model and Shimojo et al. (2000) for a jet model). Nevertheless, the MHD simulations including both reconnection and conduction have never been performed for more than the 20 years since it was first recognized that such simulations are really necessary for realistic flare modelling. This was the result of various numerical difficulties, such as anisotropic heat conductivity due to the magnetic field, and to the short conduction time, which requires implicit treatment and large computational power.

Yokoyama and Shibata (1997) succeeded, for the first time, to perform MHD numerical simulations including both reconnection and conduction. They confirmed the semi-analytical prediction by Forbes, Malherbe, and Priest (1989) that an *adiabatic slow shock is dissociated into a conduction front and an isothermal slow shock* when $t_{\rm cond} < t_{\rm A}$. Later, Chen et al. (1999) also succeeded in carrying out similar simulations. It should be stressed here that at present the

groups that succeeded to perform simulations of reconnection including heat conduction *under solar flare conditions* are only two, i.e., in Japan (Yokoyama and Shibata) and in China (Chen et al.).

Yokoyama and Shibata (1998, 2001) further extended simulations to include chromospheric evaporation. Figure 2 shows a typical example of these simulations. We can find that the adiabatic slow shock is dissociated into a conduction front and an isothermal slow shock. The outer edge of the hot cusp region, which is nearly along the magnetic field lines, is the conduction front. After the conduction front reaches the top of the chromosphere, the evaporation starts and the dense hot loop (flare loop) is created. Figure 2 shows also the theoretical soft X-ray and microwave images, which are made using the temperature and density distribution in MHD simulations and the soft X-ray filter response function, as well as the optically thin thermal free-free emissivity at 17 GHz. The cusp-shaped structure similar to the observed cusp shape of LDE flares is nicely reproduced in these theoretical soft X-ray images ($\log I_{\rm Be}$ and $\log I_{\rm thinAl}$). On the other hand, the theoretical radio image at 17 GHz ($\log I_{\rm freefree}$) does not show a bright cusp shape, which is also consistent with radio observations of LDE flares (e.g., Hanaoka 1994).

One of the most important findings of Yokoyama and Shibata's (1998, 2001) simulation is that the maximum temperature of reconnection-heated plasma (i.e., flare plasma) is given by the following formula:

$$T_{\rm max} \simeq \left(\frac{B^2 V_{\rm A} L}{\kappa_0 2\pi}\right)^{2/7} \simeq 3\times 10^7 \left(\frac{B}{50\ {\rm G}}\right)^{6/7} \left(\frac{n_0}{10^9\ {\rm cm}^{-3}}\right)^{-1/7} \left(\frac{L}{10^9\ {\rm cm}}\right)^{2/7} \quad {\rm K}, \tag{2}$$

where n_0 is the pre-flare proton number density (= electron density), L is the characteristic length of the (reconnected) magnetic loop. This relation is derived from the balance between conduction cooling $\kappa_0 T^{7/2}/(2L^2)$ (e.g., Hori et al. 1997) and reconnection heating $(B^2/4\pi)(v_{\rm A}/L)$. It was found that this formula can be applied also to stellar flares (Shibata and Yokoyama 1999).

4.3. Plasmoid (Flux Rope) Ejections

What is the triggering mechanism of solar flares and CMEs? Feynman and Martin (1995) reported interesting observations that filament eruptions (i.e., CMEs) tend to occur if emerging flux appears near the quiescent filament and if the polarity distribution of the emerging flux is favorable for magnetic reconnection with the ambient field.

Chen and Shibata (2000) succeeded in reproducing this observational tendency using an implicit MHD code developed by Hu (1989). Figure 3 shows a typical example of their simulations. Initially, they assumed a flux rope in a stable equilibrium in a 2D situation. Then, emerging flux is input from the lower boundary, which makes local reconnection just below the flux rope (filament). This small change of magnetic field configuration leads to loss of equilibrium or instability in the global system, eventually leading to eruption of the whole flux rope system. It is also possible to trigger global eruption even when emerging flux appears in a distant place from the neutral filament, if the polarity distribution is favorable for local reconnection (see Fig. 3b). Here it should be stressed that reconnection is strongly coupled to the eruption of the flux rope (filament

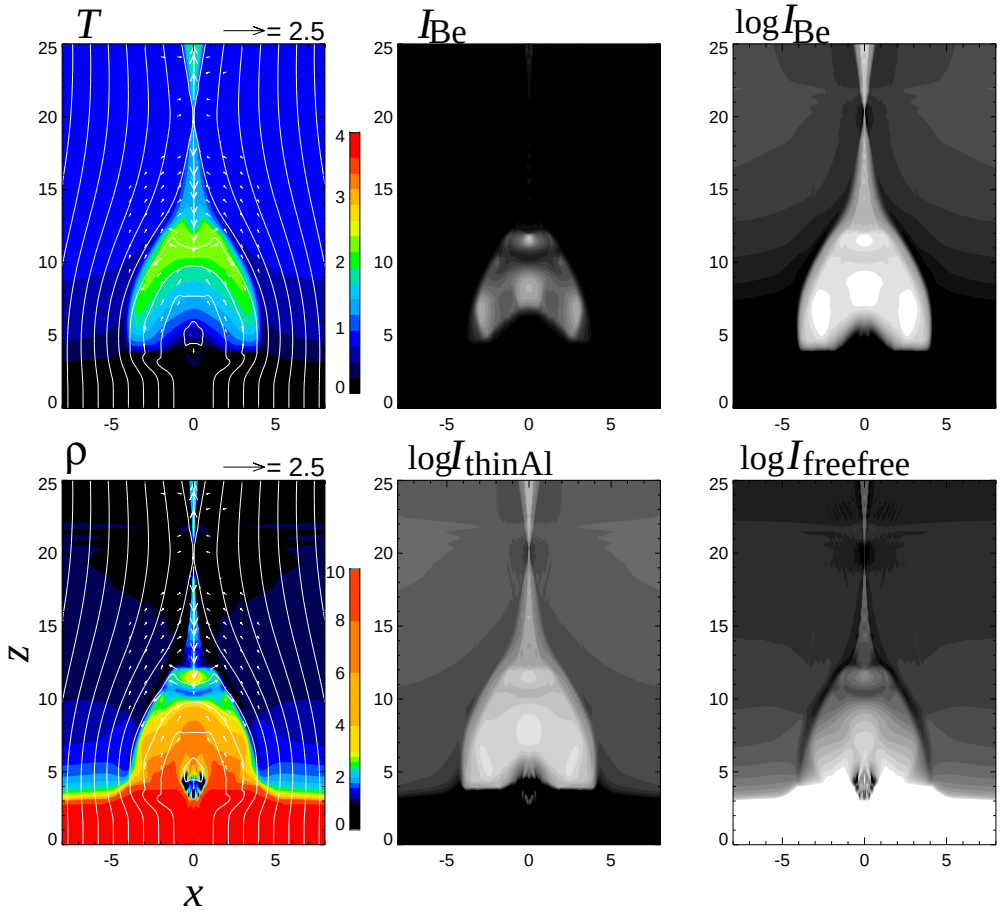

Figure 2. A typical example of MHD simulations of reconnection with heat conduction and chromospheric evaporation (Yokoyama and Shibata 1998, 2001). T and ρ show the temperature and density distributions at $t = 2.5$ (in non-dimensional units) $\simeq 450$ s. In this simulation, initially, an anti-parallel vertical magnetic field is assumed, and a dense plasma (the chromosphere) is located in the lower portion of the computational region. The Petschek-type reconnection is realized by the anomalous resistivity model. Radiative cooling and gravity are neglected, since the time scale treated in the simulations is short, corresponding to the early phase of flares. Because of the high heat conductivity, an adiabatic slow shock is dissociated into a conduction front and an isothermal slow shock, where the density jump is large. A dense thin layer with a reconnection jet emanating from the X-point corresponds to the isothermal slow shock region. Soft X-ray ($I_{\rm Be}$, $\log I_{\rm Be}$, $\log I_{\rm thinAl}$) and radio ($\log I_{\rm free-free}$) maps derived from the simulation results are shown in the middle and right panels. The radio emission is derived as thermal free-free emission. In the X-ray maps, the response of the filter attached to the soft X-ray telescope on board Yohkoh is taken into account. The unit of length, velocity, density, and temperature are 3000 km, 170 km/s, 10^9 cm^{-3} and 2×10^6 K, respectively. Note that the theoretical soft X-ray images show cusp-shaped structure similar to the actual observations of LDE flares (Tsuneta 1996).

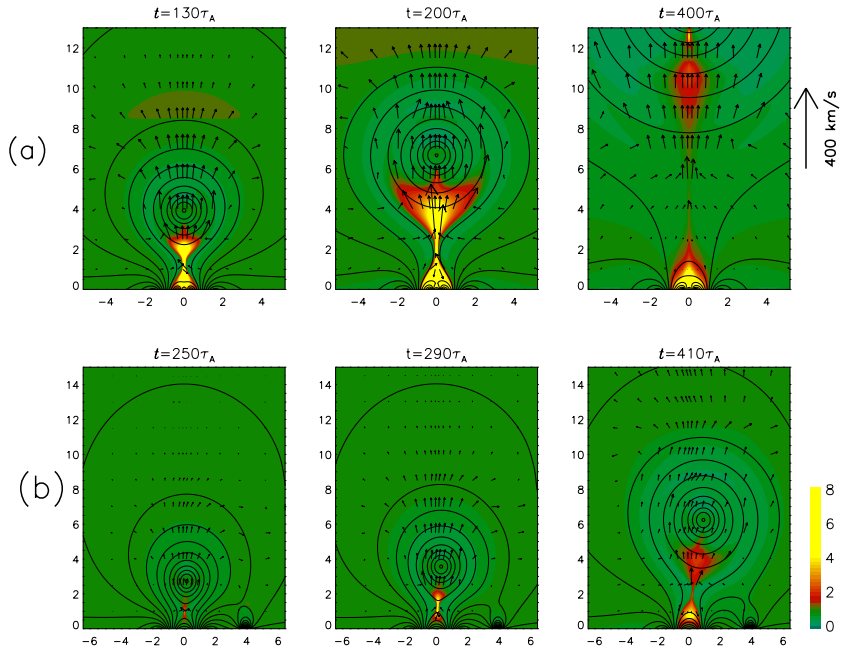

Figure 3. MHD simulations of eruption of flux rope (CME) triggered by emerging flux (Chen and Shibata 2000): two cases are shown, in which emerging flux appeared (a) just below a filament, and (b) in the distant place from the neutral line. The color map shows the temperature distribution.

or plasmoid) as discussed above. If we inhibit reconnection, the fast ejection of the flux rope cannot be possible. Since the flux rope becomes a CME itself, reconnection plays an essential role in CMEs. (See also related simulation studies by Mikic and Linker 1994, Hu 2000, Choe and Chen 2001, Kusano 2002).

5. Remaining Questions

From recent development of space observations and numerical simulations, we can now say that the magnetic reconnection mechanism is established, at least, phenomenologically. However, from physical points of view, there are a number of fundamental questions remaining:
(1) What is the condition of fast reconnection?
(2) Where are slow and fast shocks?
We still do not have firm observational evidence of these shocks. We need better observational data, as well as more realistic simulation models to compare with the observations. Namely, we have not yet developed realistic 3D models of flares/CMEs including reconnection, heat conduction and evaporation.

Furthermore, the following fundamental questions remain in relation to flares/CMEs:

(3) What is the particle acceleration mechanism in flares/CMEs?
(4) What is the energy storage and triggering mechanism of flares/CMEs?

We hope some of above questions will be solved in the near future under collaboration between advanced numerical simulations and new space solar observatories such as Solar B.

References

Aschwanden, M. et al. 2001, ARAA, 39, 175
Biskamp, D., 1986, Phys. Fluids, 29, 1520
Canfield, R. C. et al. 1996, ApJ, 464, 1016
Chen, P. F., et al. 1999, ApJ, 513, 516
Chen, P. F., and Shibata, K. 2000, ApJ, 545, 524
Choe, G. S., and Chen, C. Z. 2000, ApJ, 541, 449
Feynman, J., and Martin, S. F. 1995, JGR, 100, 3355
Forbes, T. G., Malherbe, J. M., Priest, E. R. 1989, Sol. Phys., 120, 285
Hanaoka, Y. 1994, in Proc. Kofu meeting, ed. S. Enome, and T. Hirayama, Nobeyama Radio Observatory, p. 181
Hori, K., et al. 1997, ApJ, 489, 426
Hu, Y. Q., 1989, J. Comp. Phys., 84, 441
Hu, Y. Q. 2000, Sol. Phys., 200, 115
Kusano, K. 2002, ApJ, 571, 532
Magara, T., and Shibata, K. 1999, ApJ, 514, 456
Mikic, Z. and Linker, J. 1994, ApJ, 430, 898
Scholer, M. 1989, JGR, 94, 8805
Schumacher, J. and Kliem, B. 1996, Phys. Plasmas, 3, 4703
Shibata, K., Nozawa, S., and Matsumoto, R. 1992, PASJ 44, 265
Shibata, K., et al. 1992, PASJ, 44, L173
Shibata, K. 1999, Astrophys. Sp. Sci., 264, 129
Shibata, K., and Yokoyama, T. 1999, ApJ, 526, L49
Shibata, K., and Tanuma, S. 2001, Earth, Planets, and Space, 53, 473
Shimojo, M., et al. 2001, ApJ, 550, 1051
Tajima, T., and Shibata, K. 1997, Plasma Astrophysics, Addison-Wesley
Tsuneta, S. 1996, ApJ, 456, 840
Ugai, M. 1992, Phys. Fluids B, 4, 2953
Yokoyama, T., and Shibata, K. 1994, ApJ, 436, L197
Yokoyama, T., and Shibata, K. 1995, Nature 375, 42
Yokoyama, T., and Shibata, K. 1996, PASJ 48, 353
Yokoyama, T., and Shibata, K. 1997, ApJ, 474, L61
Yokoyama, T., and Shibata, K. 1998, ApJ, 494, L113
Yokoyama, T., and Shibata, K. 2001, ApJ, 549, 1160